RASĀYAN *J. Chem.*
Vol. 19 | No. 1 | 231-243 | January-March | 2026
ISSN: 0974-1496 | e-ISSN: 0976-0083 | CODEN: RJCABP
http://www.rasayanjournal.com
http://www.rasayanjournal.co.in

VALIDATED HPLC METHOD FOR SIMULTANEOUS QUANTIFICATION OF APREPITANT AND ITS EP IMPURITIES WITH LC-MS/MS ELUCIDATION AND TOXICITY PREDICTION OF ITS FORCED DEGRADATION PRODUCTS

Katari Ravi Babu and Gowri Sankar Reddipalli✉
Department of Chemistry, GITAM School of Science, GITAM Deemed to be University, Visakhapatnam-530045, (Andhra Pradesh) India
✉Corresponding author: greddipa@gitam.edu

ABSTRACT

This present study is a validated, sensitive, and robust RP-HPLC method for real-time quantification of Aprepitant as well as its European Pharmacopoeia impurities A and B, and the proposed method was applied for a comprehensive forced degradation study through Liquid Chromatography Mass Spectrometry. Chromatographic separation was optimized utilizing a Hypersil ODS C18 (250 × 4.6 mm, 5 µm) column with equal volume isocratic elution of solvent A (45 % acetonitrile, water and solvent B (70:30 v/v composition of 0.1% formic acid (aqueous) and methanol). This method achieves effective separation of aprepitant (Rt = 6.02 min), impurity A (Rt = 3.95 min), and impurity B (Rt = 8.02 min). The method exhibits excellent sensitivity and can detect impurities up to 0.045 µg/mL. Forced degradation studies reveal that aprepitant was stable in most conditions but underwent significant degradation under alkaline stress, with the formation of five degradation products. The method resolves these newly formed DPs at retention times of 1.907, 3.140, 4.740, 5.365, and 6.923 minutes, and these DPs were designated as DP 1 to 5, respectively. This proposed method was applied to LC-MS/MS for structural characterization of DP 1 (487.45 m/z), DP 2 (509.39 m/z), DP 3 (412.31 m/z), DP 4 (396.31 m/z), and DP 5 (438.35 m/z) based on fragmentation patterns. The in-silico toxicity assessment of characterized DPs indicates that the DPs possess varying degrees of organ-specific toxicities, such as neurotoxicity and respiratory toxicity. The study result highlights the need for cautious monitoring, structural characterization, and control of these impurities during formulation development and stability studies to ensure patient and environmental safety.

Keywords: Aprepitant, EP Impurities, HPLC Quantification, Degradation Products, Characterization.
RASĀYAN *J. Chem.*, Vol. 19, No.1, 2026

INTRODUCTION

Aprepitant (Fig.-1) is a selective neurokinin-1 receptor antagonist and was widely utilised to prevent both chemotherapy-induced as well as postoperative nausea and vomiting. It inhibits the substance P binding, which is a key neuropeptide involved in emetic signalling, to neurokinin-1 receptors located in the central nervous system and provides effective control of both severe and delayed phases of emesis.[1] It exhibits high specificity, possesses a favourable pharmacokinetic profile and hence becomes a cornerstone in antiemetic therapy, especially in oncology care. Aprepitant is generally well-tolerated but may cause some side effects in some individuals, like all medications.[2] The most common adverse effects associated with the use of Aprepitant include fatigue, dizziness, hiccups, constipation, and diarrhoea. Some patients may also experience headaches, loss of appetite, or gastrointestinal disturbances, such as nausea and abdominal pain. The hypersensitivity reactions, such as rash, pruritus, or anaphylaxis, were also reported in rare cases.[3] Chemically, Aprepitant is a complex triazole derivative that contains multiple functional groups that not only contribute to its activity but are also susceptible to degradation under different stress conditions. The stability of Aprepitant and the nature of its degradation products (DPs) possess critical importance to ensure its safety and efficacy.[4] The regulatory guidelines, such as ICH Q3B (R2), emphasise the identification, quantification, and toxicological assessment of impurities and DPs that arise under forced degradation studies.[5] The survey of available analytical methods suggests the presence of

various analytical methods for the quantification of Aprepitant in various samples. Analytical HPLC methods reported for quantification of Aprepitant in pharmaceutical formulations[6-10] and LC-MS/MS reported for its assessment in biological samples.[11] The method suitable for quantification of ester and morpholine impurities of Aprepitant was also reported in the literature.[12-13] A quality-by-design-based HPLC method was reported for the evaluation of p-toluenesulfonate impurities of Aprepitant.[14] There is no method available for the quantification of European Pharmacopoeia (EP) impurities of Aprepitant. These impurities are officially recognized as unwanted substances that may be present in a drug substance or formulation. The identification and quantification of these impurities was considered as very crucial to ensure the safety, efficacy, and quality of pharmaceutical products. There is no analytical method reported for the resolution and structural characterization of DPs of Aprepitant and highlighting a significant gap in the literature. Development of a reliable and validated HPLC method for quantification of EP-specified impurities as well as DPs was essential to address this need. Hence, this present work was aimed at fulfilling the existing gap by developing and validating a robust, sensitive, and stability-indicating HPLC method for the real-time quantification of Aprepitant and its EP-specified impurities. Additionally, the study targets the structural characterization of unknown DPs formed under recommended ICH forced degradation conditions using LC-MS/MS. Further, the in-silico toxicity prediction to assess the possible risk associated with the DPs makes the method appropriate for routine quality control and stability studies. The structural details of Aprepitant and its EP impurities were given in Fig.-1.

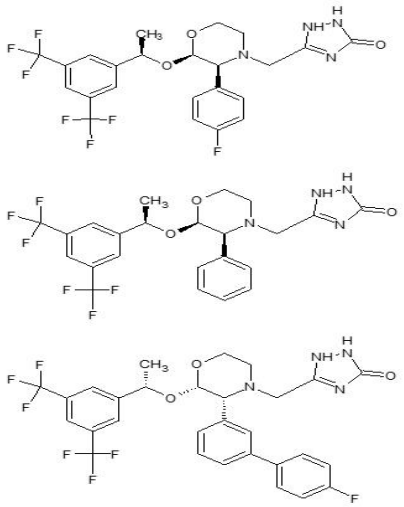

Name: Aprepitant
IUPAC name: *5-([(2R,3S)-2-((R)-1-[3,5-Bis(trifluoromethyl)phenyl]ethoxy)-3-(4-fluorophenyl)morpholino]methyl)-1H-1,2,4-triazol-3(2H)-one*
Mass: 534.435 g/mol
Formula: $C_{23}H_{21}F_7N_4O_3$.

Name: Aprepitant EP Impurity A
IUPAC name: *5-[[(2R,3S)-2-[(1R)-1-[3,5-Bis(trifluoromethyl)phenyl]ethoxy]-3-phenylmorpholin-4-yl]methyl]-1,2-dihydro-3H-1,2,4-triazol-3-one*
Mass: 516.4 g/mol
Formula: $C_{23}H_{22}F_6N_4O_3$

Name: Aprepitant EP Impurity B
IUPAC name: *5-[[(2R,3S)-2-[(1R)-1-[3,5-Bis(trifluoromethyl)phenyl]ethoxy]-3-(4'-fluorobiphenyl-3-yl)morpholin-4-yl]methyl]-1,2-dihydro-3H-1,2,4-triazol-3-one*
Mass: 610.5 g/mol
Formula: $C_{29}H_{25}F_7N_4O_3$

Fig.-1: Structure and Identification Details of Aprepitant and its EP Impurities in the Study

EXPERIMENTAL

Samples and Reagents

Aprepitant and its related substances (EP Impurity A and EP Impurity B) were obtained from Glenmark Pharmaceuticals, India, and were used as received. High-purity acetonitrile (MS grade) was sourced from Sigma Aldrich (Brazil). AR grade hydrochloric acid (HCl), sodium hydroxide (NaOH), and hydrogen peroxide (H_2O_2) were obtained from Merck (Germany). Deionized water was generated using the Direct-Q 3UV system with an integrated pump (Millipore, France). Aprepitant stock solution was formulated in acetonitrile at a concentration of 1000 µg/mL, and reference solutions of EP Impurity A and EP Impurity B were prepared at concentrations of 100 µg/mL.

Degradation Solutions

Acid Degradation Solution

The degradation behaviour of Aprepitant was examined according to the ICH Q1A (R2) stability guidelines. The active substance was exposed to several stress environments, including acidic, alkaline, and neutral hydrolysis, as well as oxidative, heat-induced, and light-induced breakdown. Experimental conditions were adjusted to achieve approximately 10 – 15 % degradation so that the resulting pathways

could be properly assessed. Quantification was carried out using HPLC with detection at 227 nm, and the resulting degradation compounds were characterized by LC-MS/TOF.

Base Degradation Solution

Hydrolytic breakdown was carried out by mixing 1 mL of 1 N HCl, 1 N NaOH, or aqueous solution with 1 mL of the Aprepitant solution, followed by heating at 80°C for 12 hours. After the reaction period, acidic mixtures were adjusted to neutral pH using an equivalent amount of base, and basic mixtures were neutralized using acid.[15]

Peroxide Degradation Solution

Peroxide degradation was performed by the combination of 1 mL of the drug solution (1000 µg/mL) and 1 mL of 10% hydrogen peroxide (H_2O_2), followed by allowing the reaction to run at room temperature for 24 hours.

Thermal Degradation Solution

Thermal degradation was performed by heating the solid drug in a sealed glass ampoule to 80 °C in a hot air oven for 7 days, with an ambient condition control sample.

UV Degradation Solution

Photostability testing was carried out in both the solid and solution forms. The powdered drug and its 1000 µg/mL solution were exposed to 1.25 million lux-hours of fluorescent illumination and 200 Wh/m² of ultraviolet light. Control samples were protected with aluminum foil to prevent light exposure. The solution form exhibited significant degradation under photolytic conditions, while the solid form was stable.

HPLC Instrumentation

The HPLC–PDA setup (Shimadzu, Kyoto, Japan) included an in-line degassing unit (DGU-20S5), a dual-pump system (LC-20AT), a communication controller (CBM-20A), coupled with an autosampler (SIL-20A), a temperature-controlled column chamber (CTO-10ASVP), and a PDA (M20A) detector capable of scanning from 190 to 800 nm. Data collection and analysis were performed using LC Solutions version 1.21 SP1 software. Analysis of HPLC-MS was conducted on an in-line system consisting of a Waters Alliance® 2695 HPLC separations module linked to a QTrap 2000 AB Sciex (mass spectrometer) with an electrospray ionization (ESI) source. The ESI source was in positive ion mode [ESI (+)], which is appropriate for ionizing moderately polar to polar analytes, including drug compounds. The temperature of the source was kept at 623 K (about 350 °C) to ensure efficient desolvation and ionization of the eluting analytes. A transfer (capillary) voltage of 4500 V was used to help facilitate ion generation and transmission from the ESI source into the mass analyzer. The system was optimized for improved sensitivity and selectivity in the detection of both Aprepitant and its EP impurities or degradation products (DPs). Chromatographic separations were conducted on a Hypersil ODS (C18) 250 mm column on both HPLC-PDA and HPLC-MS platforms. An isocratic elution was employed with the mobile phase consisting of equal volumes of Solvent A (acetonitrile and water (45:55)) and B (0.1% formic acid with methanol (70:30)) at a flow rate of 0.8 mL/min, and 20 µL injection volume for both systems.

LC-MS/MS Analysis

To investigate the fragmentation patterns of protonated Aprepitant and its EP-related impurities, tandem mass spectrometry was carried out using a Q-TOF system (Micromass, U.K.) operating in +ESI mode. Data were acquired in the m/z range of 50–1000 to enable comprehensive detection of potential fragment ions. Samples were injected directly into the MS at a constant rate of 10 µL/min via a syringe pump, ensuring consistent ion introduction. High-purity nitrogen was supplied at 1.5 L/min, serving as both the nebulizing and auxiliary gas to facilitate solvent removal. Capillary voltage was maintained at 3.0 kV, while the cone voltage was set at 35 V to optimize ion transmission and minimize undesired fragmentation. The desolvation curved line and heat block was held at 373 K (100 °C) to promote efficient solvent evaporation and maintain ion stability during transport. Collision-induced dissociation of selected precursor ions was carried out using argon as the collision gas. The collision energy and pressure

were optimally regulated to cause extensive and reproducible fragmentations of the precursor ion, which assisted in effective structural elucidation of Aprepitant along its EP impurities and DPs.[17]

Method Development and Validation

Method development entailed rigorous optimization of mass spectrometric and chromatographic conditions to obtain effective separation, precise quantitation, and accurate identification of Aprepitant and its associated impurities or DPs. Important parameters like flow rate, mobile phase composition, detection wavelength, and pH were investigated.[18]

Method Validation

Specificity: Specificity was predictable by injecting the degradation solution into the LC-MS, which displayed an outstanding mass purity for Aprepitant along with its EP impurities and DPs.

Linearity: Six replicates of six concentrations over of 15 to 90 µg/mL range were used for the linearity study. Aprepitant and its EP impurities achieved a linear response.

Precision: For precision, the method was considered at intra-day and Inter-day by analyzing single concentrations at three replicates of Aprepitant and its EP impurities. The result was expressed in RSD% %.

Accuracy: Accuracy was evaluated by employing a replicated experiment at three different levels, 50 % which is 45 µg/mL, 100 % which is 60 µg/mL; and 150 % which is 75 µg/mL. The concentration by addition of the standard solution in Aprepitant and its EP impurities. At each level, the % of drug recovery was considered.

Sensitivity: LOD and LOQ were calculated according to the signal-to-noise ratio and were calculated according to chromatographic conditions.

Robustness: Method robustness was examined by persistently changing experimental key parameters for Aprepitant at a 60 µg/mL solution was analyzed at ±5 mL flow rates (0.85 and 0.75 mL/min) and wavelengths (215 and 205 nm).[19]

***In-silico* Toxicity Studies**

The toxic potential of the DPs was assessed through an *in-silico* prediction of toxicity. This was done using ProTox-II, a well-established web application used to predict the toxicological profiles of chemical entities based on their molecular structure. ProTox-II estimates the median lethal dose (LD_{50}), as the dose (in mg/kg body weight) administered to kill 50% of a test population, and thus gives a quantitative estimate of acute toxicity. Besides LD_{50} values, the program assigns compounds into toxicity class from Class 1 (most toxic) to Class 6 (least toxic), which gives an idea of qualitative potential health risk. These forecasts provide invaluable information regarding the safety profile of Aprepitant and its DPs, particularly under conditions favouring degradation, for example, environmental exposure or long-term storage.

RESULTS AND DISCUSSION

Degradation Study

Forced degradation study of Aprepitant was analyzed by HPLC-PDA. Aprepitant displays one DP in the acid and peroxide degradation study, but in base degradation, it shows 5 DPs. In the base degradation process, identified DPs retention time and acid and peroxide degradation compounds retention time is the same, so according to this total of five DPs are identified in the degradation process. So, in the base degradation process total of five DPs are identified and named as DP 1- DP 5 according to the elution time. Overlay chromatogram of the degradation study is given in Fig.-2.

Characterization of DPs by LC-MS/MS

Although degradation was performed under acidic, basic, peroxide, thermal and UV conditions, the DPs were identified only under basic conditions, indicating that the base played a significant role in the degradation pathway. In base degradation Total of 5 DPs are identified, retention time of the DPs are

1.907 mins (DP1), 3.140 mins (DP2), 4.740 mins (DP3), 5.365 mins (DP4), and 6.923 mins (DP5), along with Aprepitant. No other impurities or disturbances was observed in the study.

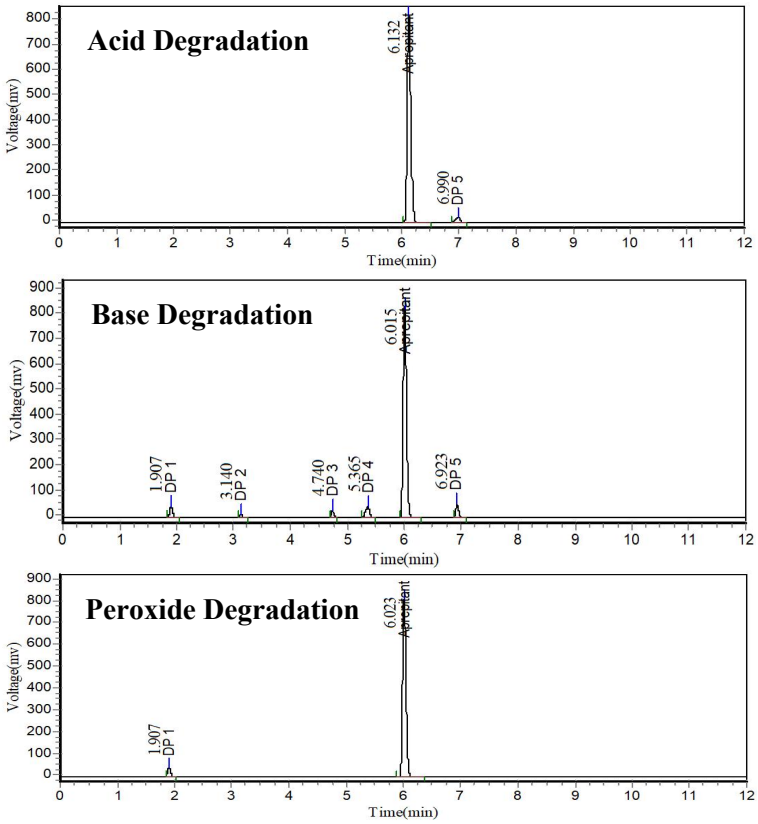

Fig.-2: Forced Degradation Study Chromatograms Observed for the Study

DP 1 Characterization

DP 1 molecular weight of the compound is m/z 487.4497 $[M+1]^+$ with representing the molecular formula $C_{23}H_{23}FN_4O_7$. Parent ion forms three production ions with m/z of 440.4158, 191.1931, and 170.1541 $[M+1]^+$ by the loss of CH_3O_2, $C_{12}H_{14}N_3O_6$, $C_{15}H_{14}FN_4O_3$ and resulted fragments with formula of $C_{22}H_{20}FN_4O_5$, $C_{11}H_9FNO$, and $C_8H_9O_4$. Precursor ion of $C_{22}H_{20}FN_4O_5$ forms another two product ions by the loss of $C_9H_6O_4$, and $C_{11}H_8O_4$ formed fragments with masses 262.2743 m/z ($C_{13}H_{14}FN_4O$), 236.2370 ($C_{11}H_{12}FN_4O$). Product ion of m/z 236.2370 loss C_6H_3F and forms $C_5H_9N_4O$ (m/z 142.1506). By fragmentation mechanism DP 1 was identified as *5-((R)-1-(((2R,3S)-3-(4-fluorophenyl)-4-((5-oxo-2,5-dihydro-1H-1,2,4-triazol-3-yl)methyl)morpholin-2-yl)oxy)ethyl)isophthalic acid*. DP 1 fragmentation mechanism is given in Fig.-3, mass spectra are given in Fig.-4, and MS/MS data was tabulated in Table-1.

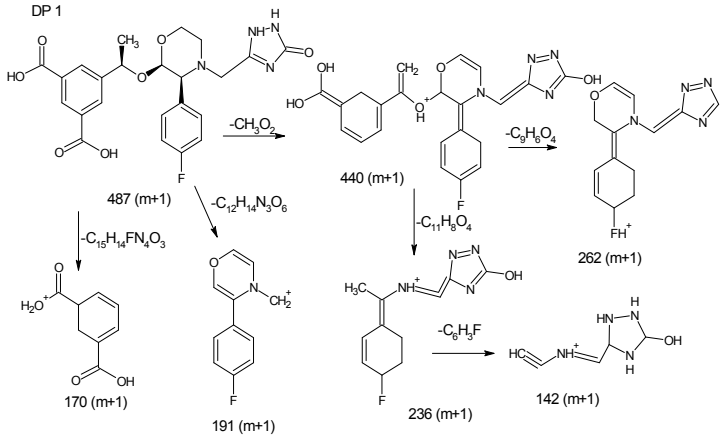

Fig.-3: DP 1 Fragmentation Mechanism

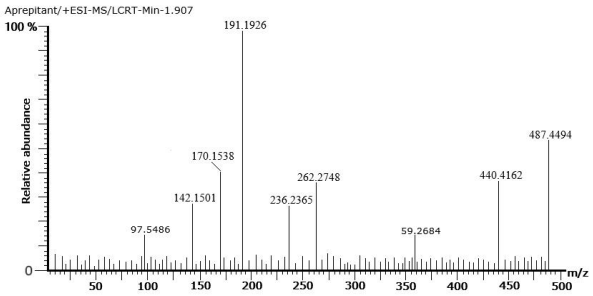

Fig.-4: DP 1 Mass Spectra

Table-1: MS/MS Data Observed for DP 1

Observed mass (m/z) (m+1)	Molecular Formula	Calculated mass (m/z) (m+1)	Error (ppm)	RDB	Structure
487.4494	$C_{23}H_{23}FN_4O_7$	487.4497	-0.615	14.0	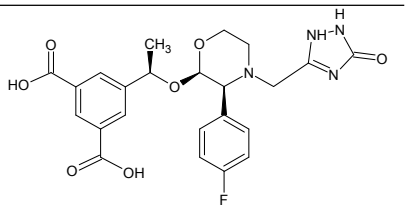
440.4162	$C_{22}H_{20}FN_4O_5$	440.4158	0.908	14.5	
262.2748	$C_{13}H_{14}FN_4O$	262.2743	1.906	8.5	
236.2365	$C_{11}H_{12}FN_4O$	236.2370	-2.117	7.5	
191.1926	$C_{11}H_9FNO$	191.1931	-2.615	7.5	
170.1538	$C_8H_9O_4$	170.1541	-1.763	4.5	
142.1501	$C_5H_9N_4O$	142.1506	-3.517	3.5	

DP 2 Characterization

DP 2 was identified at 3.140 mins in the base degradation study with a mass of m/z 509.3893 $[M+1]^+$, and the formula is $C_{21}H_{19}F_7N_4O_3$. Parent ion forms three precursor ions by the reduction of $C_2H_2N_3O_2$, $C_{13}H_{12}F_6N_3O_2$, and $C_{18}H_{17}F_7NO_3$. formed fragment ions are with mass of m/z 409.3326 ($C_{19}H_{17}F_7NO$), 153.1451 (C_8H_7FNO) and 81.0675 ($C_3H_2N_3$) $[M+1]^+$. Product ion of 409.3326 m/z forms another precursor ion by the reduction of C9H10FNO. The resulting product ion is m/z 242.1524 ($C_{10}H_7F_6$), which forms a precursor ion that loses CHF_3 and forms the last product ion with a mass of m/z 172.1386 ($C_9H_6F_3$). By all this fragmentation pattern, DP 2 was identified as *5-((((1S,2R)-2-(®-1-(3,5-bis (trifluoromethyl) phenyl)ethoxy) -1-(4-fluorophenyl) -2-hydroxyethyl) amino) methyl)-1H-1,2,4-triazol-3(2H)-one*. DP 2 fragmentation mechanism is given in Fig.-5, mass spectra are given in Fig.-6. And MS/MS data was tabulated in Table-2.

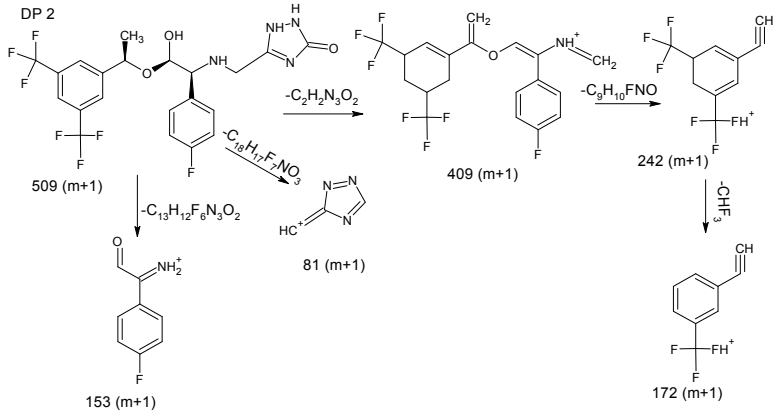

Fig.-5: DP 2 Fragmentation Mechanism

DP 3 Characterization

DP 3 is identified at 4.740 mins in the base degradation with 412.3139 m/z of mass and $C_{18}H_{16}F_7NO_2$ of molecular formula. Parent ion of 412.3139 m/z forms three product ions by the reduction of H_4NO, $C_{10}H_8F_6N$, and $C_{10}H_9F_6O_2$. The resulting fragment ions' mass is m/z 378.2755, 156.1457, 137.1457 with molecular formulas of $C_{18}H_{12}F_7O$, $C_8H_8FO_2$, C_8H_7FN.

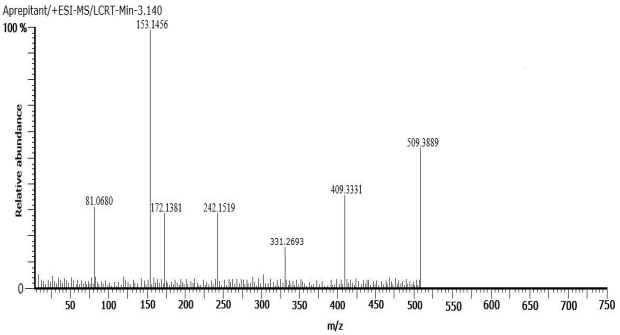

Fig.-6: DP 2 Mass Spectra

Table-2: MS/MS Data Observed for DP 2

Observed mass (m/z) (m+1)	Molecular formula	Calculated mass (m/z) (m+1)	Error (ppm)	RDB	Structure
509.3889	$C_{21}H_{19}F_7N_4O_3$	509.3893	-0.785	11.0	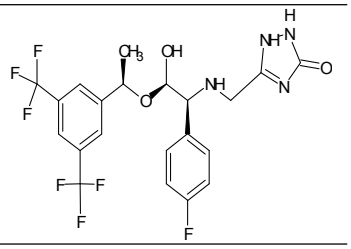
409.3331	$C_{19}H_{17}F_7NO$	409.3326	1.222	8.5	
242.1519	$C_{10}H_7F_6$	242.1524	-2.065	4.5	
172.1381	$C_9H_6F_3$	172.1386	-2.905	20.5	
153.1456	C_8H_7FNO	153.1451	1.306	5.5	
81.0680	$C_3H_2N_3$	81.0675	6.168	4.5	

Fragment ion of m/z 378.2755 ($C_{18}H_{12}F_7O$) produces another two precursor ions by the reduction of C_8H_3FO, and $C_9H_4F_4$ resulted ions mass is m/z 244.1683 ($C_{10}H_9F_6$), and 190.1538 ($C_9H_8F_3O$). Precursor ion of m/z 244.1683 loses C_2H_4 and forms a fragment ion with $C_8H_5F_6$ (m/z 216.1151), another fragment of m/z 190.1538 loses H_4O and forms a product ion with mass of m/z 170.1227 ($C_9H_4F_3$). Precursor ion of m/z 137.1457 lost C_2HN, and the resulting fragment is m/z 98.1096 of mass and C_6H_6F is the molecular formula. By all this fragmentation pattern, DP 3 was identified as *(1R,2S)-2-amino-1-{(1R)-1- [3,5-bis(trifluoromethyl)phenyl]ethoxy} -2-(4-fluorophenyl) ethanol*. DP 3 fragmentation mechanism is given in Fig.-7, mass spectra are given in Fig.-8 and MS/MS data was tabulated in Table-3.

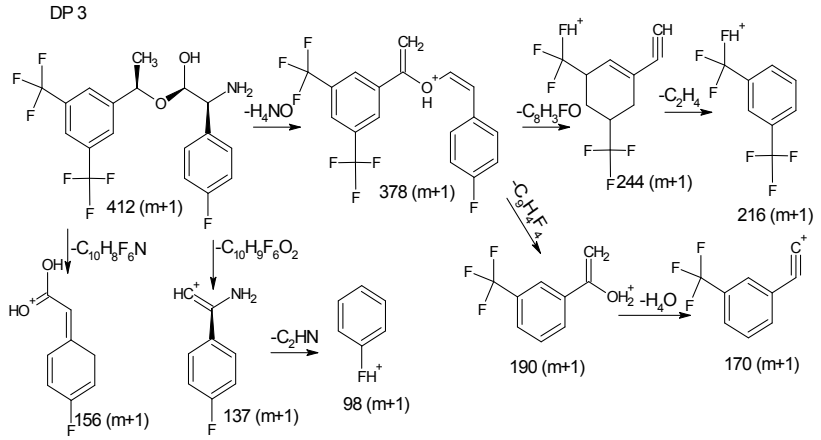

Fig.-7: DP 3 Fragmentation Mechanism

DP 4 Characterization

DP 4 is observed at 5.365 mins with m/z 396.3145 $[M+1]^+$ with molecular formula of $C_{18}H_{16}F_7NO_2$. Product ions of DP 4 are m/z 272.1784 ($C_{11}H_9F_6O$), 240.1613 ($C_{10}H_8F_5O$), 170.1227($C_9H_4F_3$), 125.1350 (C_7H_7FNO). By this fragmentation pattern DP 4 was identified as *(1S)-2-{(1R)-1-[3,5-bis(trifluoromethyl)phenyl]ethoxy}-1-(4-fluorophenyl)ethanamine*. DP 4 fragmentation mechanism is given in Fig.-9, mass spectra are given in Fig.-10. And MS/MS data was tabulated in Table-4.

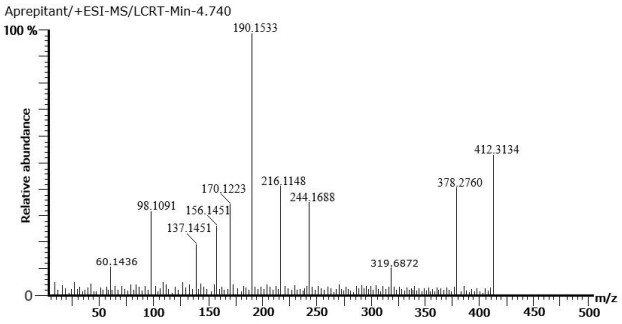

Fig.-8: DP 3 Mass Spectra

Table-3: MS/MS Data Observed for DP 3

Observed mass (m/z) (m+1)	Molecular formula	Calculated mass (m/z) (m+1)	Error (ppm)	RDB	Structure
412.3134	$C_{18}H_{16}F_7NO_2$	412.3139	-1.213	8.0	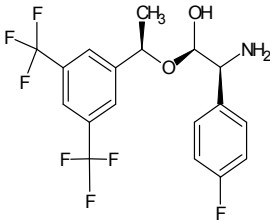
378.2760	$C_{18}H_{12}F_7O$	378.2755	1.322	9.5	
244.1688	$C_{10}H_9F_6$	244.1683	2.048	3.5	
216.1148	$C_8H_5F_6$	216.1151	-1.388	3.5	
190.1533	$C_9H_8F_3O$	190.1538	-2.629	4.5	
170.1223	$C_9H_4F_3$	170.1227	-2.351	6.5	
156.1451	$C_8H_8FO_2$	156.1457	-3.843	4.5	
137.1451	C_8H_7FN	137.1457	-4.375	5.5	
98.1091	C_6H_6F	98.1096	-5.096	3.5	

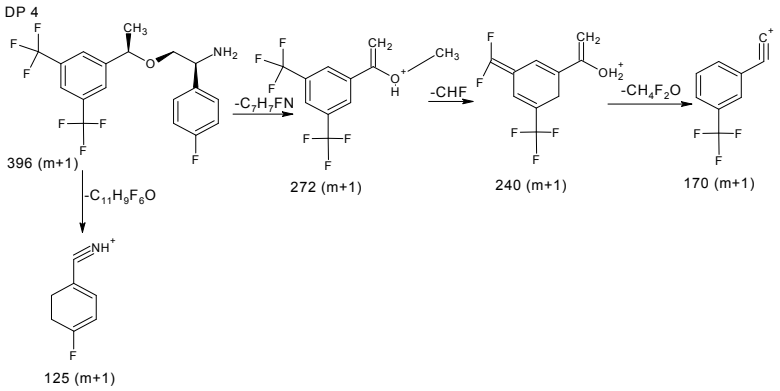

Fig.-9: DP 4 Fragmentation Mechanism

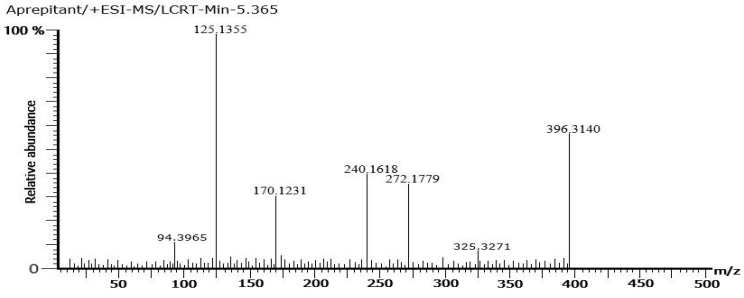

Fig.-10: DP 4 Mass Spectra

DP 5 Characterization

DP 5 is identified in both acid degradation study and base degradation study with 6.9 mins of retention time with mass of m/z 438.3512 $[M+1]^+$ representing molecular formula is $C_{20}H_{18}F_7NO_2$. Product ions formed in the DP 5 are m/z 299.3309 ($C_{18}H_{18}F_6NO_2$), 240.1365 ($C_{10}H_5F_6$), 163.1830 ($C_{10}H_9FN$), 139.1616 (C_8H_9FN), 110.1203 (C_7H_6F), 102.1247 (C_8H_5). By this fragmentation pattern DP 5 was identified as *(2R,3S)-2-{(1R)-1-[3,5-bis(trifluoromethyl)phenyl]ethoxy}-3-(4-fluorophenyl)morpholine*. DP 5 fragmentation mechanism is given in Fig.-11, mass spectra are given in Fig.-12. And MS/MS data was tabulated in Table-5.

Table-4: MS/MS Data Observed for DP 4

Observed mass (m/z) (m+1)	Molecular formula	Calculated mass (m/z) (m+1)	Error (ppm)	RDB	Structure
396.3140	$C_{18}H_{16}F_7NO_2$	396.3145	-1.262	8.0	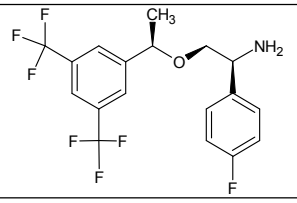
272.1779	$C_{11}H_9F_6O$	272.1784	-1.837	4.5	
240.1618	$C_{10}H_8F_5O$	240.1613	2.082	4.5	
170.1231	$C_9H_4F_3$	170.1227	2.351	6.5	
125.1355	C_7H_7FNO	125.1350	3.996	4.5	

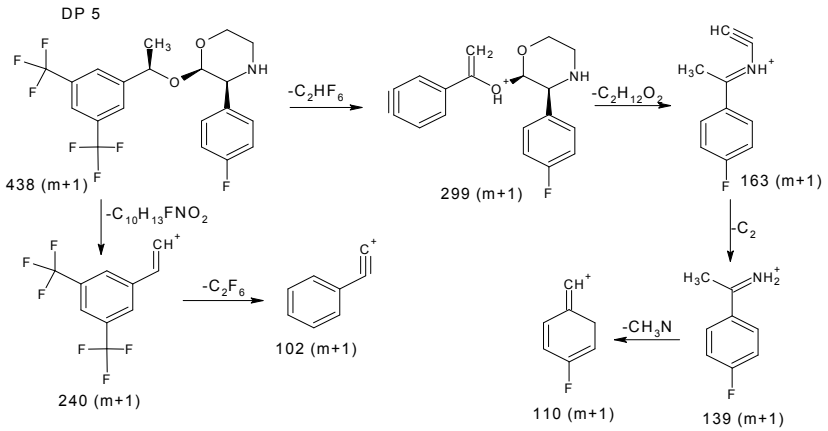

Fig.-11: DP 5 Fragmentation Mechanism

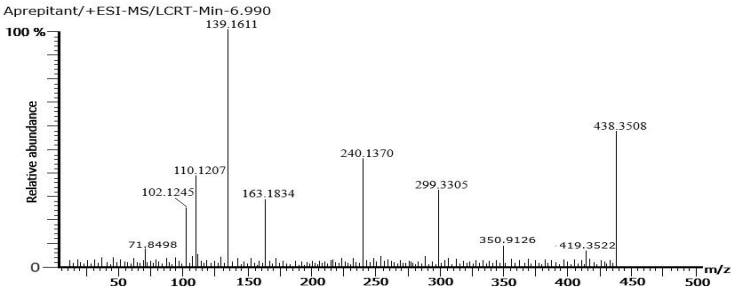

Fig.-12: DP 5 Mass Spectra

Table-5: MS/MS Data Observed for DP 5

Observed mass (m/z) (m+1)	Molecular formula	calculated mass (m/z), (m+1)	Error (ppm)	RDB	Structure
438.3508	$C_{20}H_{18}F_7NO_2$	438.3512	-0.913	9.0	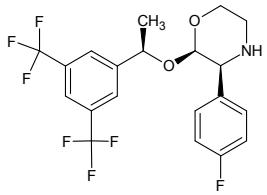
299.3305	$C_{18}H_{18}F_6NO_2$	299.3309	-1.336	7.5	
240.1370	$C_{10}H_5F_6$	240.1365	2.082	5.5	
163.1834	$C_{10}H_9FN$	163.1830	2.451	6.5	
139.1611	C_8H_9FN	139.1616	-3.593	4.5	
110.1207	C_7H_6F	110.1203	3.632	4.5	
102.1245	C_8H_5	102.1247	-1.958	6.5	

Method Development

In method development trial 1 (Fig.-13A), was Hypersil ODS (C18) 250 mm column was employed with a 90:10 ratio of methanol and acetonitrile, with 210 nm wavelength detection and 0.8 mL/min flow rate. In these conditions, merged peaks with a disturbed baseline were observed, so we continued to another with a change of mobile phase. In trial 2, Fig.-13B, the Mobile phase was changed to methanol and water 50:50 ratio, under these conditions's impurity peaks are merged, so these conditions are not suitable for the optimization to continue to another trial. In trial 3, Fig.-13C, The Mobile phase changed to methanol, acetonitrile and water with a ratio of 70:20:10 v/v. In this trial EP impurity peak was separated, but the EP impurity B was not separated properly. In trial 4, Fig.-13D, Acetonitrile, 0.1% aqueous acetonitrile and methanol was prepared. In this trial, peaks representing the EP impurity A, Aprepitant, and EP impurity B was separated, but resolution was not within the acceptable limit.

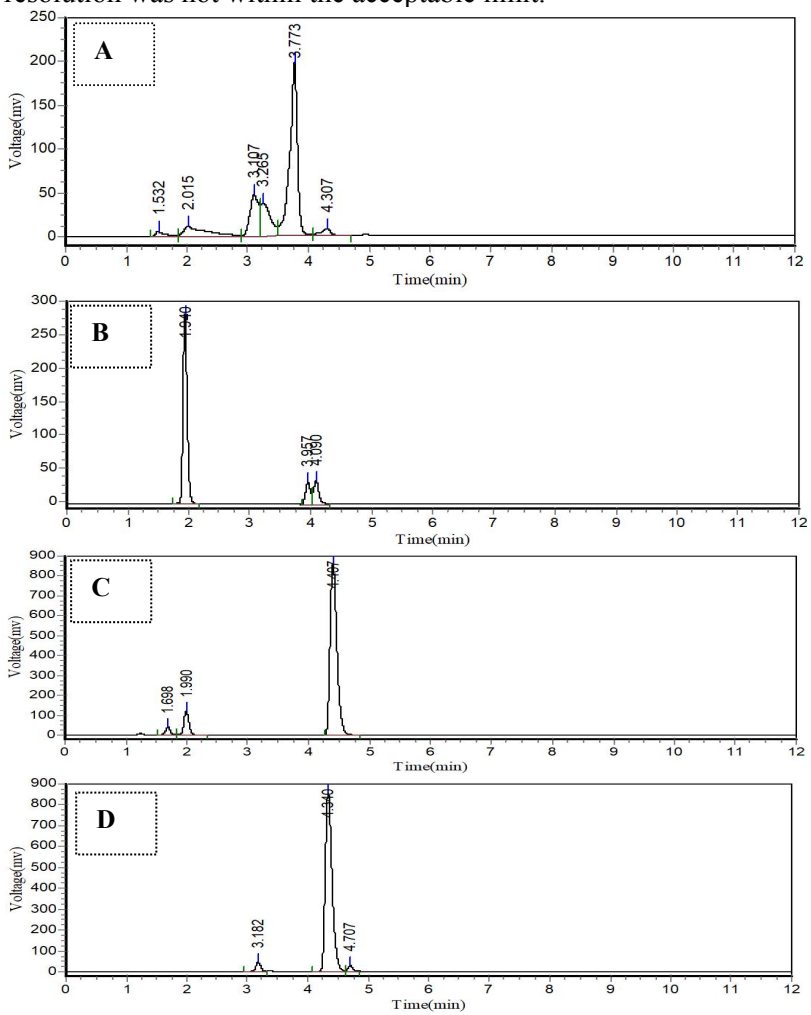

Fig.-13: Method Development Chromatograms Observed for Aprepitant, and its Impurities in the Study

Then trying with different ratios of mobile phase finally the mobile phase was prepared with solvent A and Solvent B in 50:50 v/v ratio, Solvent A consist of acetonitrile and water in the proportion 45:55 (v/v), Solvent B consist of 0.1 % Formic acid and methanol in 70:30 ratio of (v/v), in these conditions EP impurity A, Aprepitant, and EP impurity B was separated and system suitability parameters like theo plates, tail factor and resolution are in the acceptable limit. The final optimized chromatographic conditions involved the use of a Hypersil ODS 250 mm C18 column operated at ambient temperature with both HPLC-PDA & HPLC-MS systems. Separation was achieved under isocratic conditions, with a mobile phase prepared by mixing Solvent A (acetonitrile and water (45:55)) and Solvent B (0.1% formic acid and methanol (70:30)) in a 50:50 (v/v) ratio, at 0.8 mL/min flow with 20 µL of injection volume.

Method validation

The developed and optimized chromatographic method for the study of Aprepitant and its related EP impurities demonstrates satisfactory separation and analytical performance. Aprepitant was eluted at a Rt of 6.02 min, whereas impurity A & B were identified at 3.95 min and 8.02 min, respectively, Fig.-14. The absence of these peaks in chromatograms obtained from placebo and blank samples confirms the method specificity. The method system suitability was evaluated to ensure performance consistency of the chromatographic system. The theoretical plate count was found to be greater than 4000 for all three analytes, indicating good column efficiency. The tailing factor was observed to be less than 1.5 reflects acceptable peak symmetry, whereas the resolution between aprepitant and its impurities was consistently more than 2.0, confirming adequate separation and reliability of quantification under the selected chromatographic conditions.

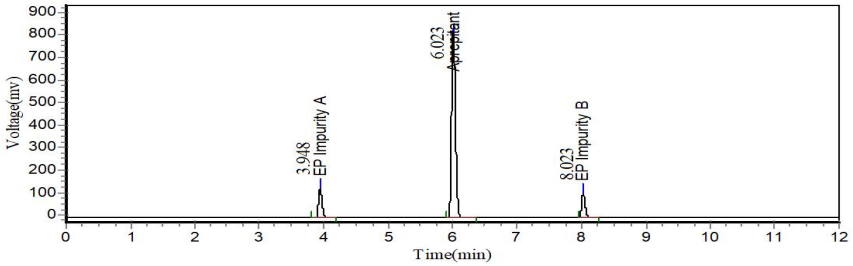

Fig.-14: System Suitability Chromatogram Observed in the Proposed Method

Method linearity was established at linear concentrations of 15 – 90 µg/mL for aprepitant and 0.15 – 0.9 µg/mL for both impurities. The calibration curve shows excellent correlation with regression equation of $y = 37684x + 129689$ ($R^2 = 0.9983$) for Aprepitant, $y = 540337x + 9101.5$ ($R^2 = 0.9996$) for impurity A, and $y = 447634x + 8262.4$ ($R^2 = 0.9973$) for impurity B. This result confirms the reliability and suitability of the method for quantitative analysis of aprepitant and its EP impurities with high specificity and strong linear response across the tested concentration range. Precision method was evaluated through intraday and interday repeatability, as well as ruggedness assessments, and the results demonstrate the method's reliability and reproducibility. Intra-day precision, which was expressed as %RSD and was found to be 1.21% for Aprepitant, 0.75% for EP impurity A, and 1.06% for EP impurity B. The result indicates excellent repeatability within a single analytical run. The inter-day precision result was similarly consistent with a %RSD of 1.23% for Aprepitant, 1.00% for impurity A, and 0.92% for impurity B, confirming the method's stability over multiple days and across different runs. The ruggedness of the method was tested by analyzing the same samples under different laboratory conditions, such as different analysts, and yielded a %RSD of 1.07% for Aprepitant, 0.76% for impurity A, and 0.97% for impurity B. These results further support the robustness and reproducibility of the method. The achieved %RSD values were well within the generally accepted limits of less than 2.0%, demonstrating that the method displays consistent and reproducible results under varied conditions. These results further affirm the method's suitability for reliable routine analysis of aprepitant and its EP impurities. The recovery studies conducted for Aprepitant, as well as its impurities A and B, in the proposed method confirm that the % recovery values were within the acceptable limit of 98-102 %. Moreover, the detection limit (LOD) of impurities was determined in the proposed method to assess the sensitivity, and the results demonstrate that the method detects both impurities up to 0.045 µg/mL. The sensitivity concentration indicates the method can detect impurities at even trace levels of these impurities.

***In-silico* Toxicity**

The drug DPs may exhibit clinically relevant toxicities, and some may pose ecotoxicological risks; hence, a detailed study was conducted to predict the toxicological effect of DPs characterized in this study. The *in-silico* toxicity evaluation of DP 1 to DP 5 of Aprepitant confirms that the DPs are classified under toxicity class 4 with predicted LD_{50} values in the range of 1000 to 1700 mg/kg. The toxicity class and LD_{50} concentration suggest that the DPs are moderately toxic if ingested. The DP 1 demonstrates significant potential toxicity towards the liver, nervous system, kidneys, lungs, and general clinical safety, whereas DP 2 displays less acute toxicity than DP 1 and exhibits a broader toxicity profile that includes

hepatotoxicity, neurotoxicity, nephrotoxicity, respiratory toxicity, immunotoxicity, and BBB-permeable, which makes it a significant impurity of concern. The DP 3 shows a narrower spectrum of toxicity and toxicity limited to neurotoxicity, respiratory toxicity, and cardiotoxicity, whereas DP 4 was active for neurotoxicity and respiratory toxicity, BBB permeability, and was also ecotoxic, suggesting that this DP not only poses patient health risks but also has environmental implications. Importantly, DP 5 can cross the BBB and poses an increased in central nervous system-related toxic effects. Collectively, these findings indicate that the DPs of Aprepitant do not show genotoxicity, cytotoxicity, or carcinogenicity, but several DPs may exhibit organ-specific toxicity and BBB penetration, which can have serious clinical implications. Moreover, the ecotoxic potential of DP 4 and DP 5 raises concerns about their environmental safety, particularly in waste management and pharmaceutical disposal contexts.

CONCLUSION

In the present research work, a strong, sensitive, and a validated RP-HPLC analytical method was successfully established for concurrent estimation of Aprepitant and EP impurities A and B and the effective separation of DPs developed under stress degradation conditions. The analytical method shows very good chromatographic efficiency and sensitivity that is appropriate for regulatory purposes and routine quality control. The approach shows great linearity ($R^2 > 0.997$), precision (intra- and inter-day %RSD < 1.3%), and accuracy (98–102% recovery). The sensitivity was also high, with a LOD for both impurities determined to be 0.045 µg/mL. The method exhibits compatibility with HPLC-MS, further expanding the method's utility for both quantification and structural analysis. The approach effectively identifies five DPs of Aprepitant that were generated under predominantly alkaline stress conditions and were analyzed by LC-MS/MS. No DPs are found under peroxide, thermal, or photolytic conditions that indicate the major contribution of base-catalyzed hydrolysis to the degradation process of Aprepitant. The DPs generated in the stress study show characteristic fragmentation patterns that confirm their respective chemical structures. Among the DPs characterized, DP 5 was significantly seen under both acidic and basic stress, indicating its relative stability under various conditions. The structural information obtained in this study offers an overall perception of the degradation behaviour of aprepitant, which was important to ensure its chemical stability, regulatory acceptability, and safety. The in-silico toxicity evaluation of DPs indicates moderate toxicity with organ-specificity and BBB permeability, further attesting to the possible clinical and environmental hazards that need to be cautiously monitored and regulated for DPs. Overall, the established HPLC method was stable, reliable, and appropriate for the regular quality control, impurity analysis, and stability testing of Aprepitant in pharmaceutical formulations. It meets regulatory requirements and offers a solid basis for product release and shelf-life assessment.

ACKNOWLEDGMENTS

The authors wish to acknowledge the Department of Chemistry, Gitam School of Science, GITAM Deemed to be University, Visakhapatnam, for the support to complete the research work.

CONFLICT OF INTERESTS

The authors declare that there is no conflict of interest.

AUTHOR CONTRIBUTIONS

The present work is related to *SDG-3: Good Health and Well-being*.All the authors contributed significantly to this manuscript, participated in reviewing/editing and approved the final draft for publication. The research profile of the authors can be verified from their ORCID IDs, given below:

Katari Ravi Babu https://orcid.org/0009-0005-5065-3610
Gowri Sankar Reddipalli https://orcid.org/0000-0002-5656-7220

Cite this article as: K. R. Babu and G. S. Reddipalli, *Rasayan J. Chem.*, 19(1), 231-243(2026), https://doi.org/10.317 88/RJC.2026.1919524.

REFERENCES

1. K. M. Brands, J. F. Payack, J. D. Rosen, T. D. Nelson, A. Candelario, M. A. Huffman, M. Z. Matthew, J. Li, C. Bridgette, J. S. Zhiguo, M. T. David, K. Hanse.n, P. N. Devine, J. P. Philip, R. Kai, G. D. Peter, A. R. Robert, J. W. Christopher, J. M. David, N. T. Nancy, M. M. James and J. R. Paul, *Journal of the American Chemical Society,* **125,** 2129(2003), https://doi.org/10.1021/ja027458g
2. N. M. Rupniak and M. S. Kramer, *Journal of Affective Disorders,* **223,** 121(2017), https://doi.org/10.1016%2Fj.jad.2017.07.042
3. M. Bergström, R. J. Hargreaves, H. D. Burns, M. R. Goldberg, D. Sciberras, S. A. Reines, J. P. Kevin, O. Mattias, G. Antoni, B. Långström, E. Olli, M. Mika, S. Olof, K. M. Anup, L. C Marvin, P. B. Wendy, E. B. Thomas, G. Cynthia and H. Jarmo, *Biological Psychiatry,* **55,** 1007(2004), https://doi.org/10.1016%2Fj.biopsych.2004.02.007
4. S. R. Tummala and K. P. Amgoth, *Turkish Journal of Pharmaceutical Science,* **19,** 455(2022), https://doi.org/10.4274/tjps.galenos.2021.17702
5. ICH Guideline Q3B (R2). Guideline on impurities in new drug substances. step 4 (2006).
6. K. M. Amgoth and S. R. Tummala, *Journal of Research in Pharmacy,* **26,** 1685(2022), https://doi.org/10.29228/jrp.259
7. N. Sreekanth, Z. A. Bahlul, C. H. Babu Rao and K. Mukkanti, *Recent Research in Science and Technology,* **3,** 16 (2011).
8. K. Krishna Chaitanya, D. Gowri Sankar, D. Samson Israel and C. H. Narasimha Kumar, *The Pharmaceutical Chemistry,* **5,** 39 (2013).
9. B. Suresh Babu, K. Natraj, V. Anil Kumar, K. Hussain Raviteja and M. K. Sreenivasulu, *Journal of Chemical and Pharmaceutical Research,* **5,** 181 (2013).
10. P. Geetha Swarupa, D. Radha Krishna, K. R. S. Prasad and K. Suresh Babu, *The Pharmacy Letter,* **7,** 264(2015).
11. E. Nazlı, R. Tuba, B. I. Alper, B. Erem, K. Sedef and N. Emirhan, *Bioanalysis,* **13,** 363(2021), https://doi.org/10.4155/bio-2020-0293
12. W. Di, J. P. Dustin, Z. Xianguo, D. D. Steven and S. B. Jeffrey, *Research Journal of Pharmaceutical and Biomedical Analysis,* **49,** 739(2009), https://doi.org/10.1016/j.jpba.2008.12.005
13. T. Sambasiva Rao and P. A. Krishnamanjari, *Journal of Research in Pharmacy,* **26,** 1685(2002), https://doi.org/10.29228/jrp.259
14. M. Srihari, R. Vinay and K. N. Jayaveera, *Archives of Applied Science Research,* **5,** 280 (2013).
15. K. Z. Constantinos and E. Vastardi, *Journal of Pharmaceutical and Biomedical Analysis,* **150,** 152(2018), https://doi.org/10.1016/j.jpba.2017.12.009
16. T. Sambasiva Rao, G. Naveena and T. Hemant Kumar, *Current Pharmaceutical Analysis,* **20,** 944(2024), https://doi.org/10.2174/0115734129332940240919113159
17. S. S. Prasad, B. B. Kasimala and V. R. Anna, *Rasayan Journal of Chemistry,* **14(4),** 2183(2021), http://doi.org/10.31788/RJC.2021.1446426
18. B. Ravinder, T. Hemant Kumar, P. Vijay Srinivas, A. Likhitha, T. Sambasiva Rao and G. Naveena, *Letters in Applied NanoBioScience,* **14,** 1 (2024), https://doi.org/10.33263/LIANBS141.048
19. B. B. Kasimala, V.R. Anna and U.R Mallu, *The Pharmacy Letter,* **6,** 411(2024).

[RJC-9524/2025]